

Physical constraints on epistasis

Kabir Husain¹ and Arvind Murugan^{1,*}

¹*James Franck Institute and the Department of Physics, University of Chicago, Chicago IL, USA*

Living systems evolve one mutation at a time, but a single mutation can alter the effect of subsequent mutations. The underlying mechanistic determinants of such epistasis are unclear. Here, we demonstrate that the physical dynamics of a biological system can generically constrain epistasis. We analyze models and experimental data on proteins and regulatory networks. In each, we find that if the long-time physical dynamics is dominated by a slow, collective mode, then the dimensionality of mutational effects is reduced. Consequently, epistatic coefficients for different combinations of mutations are no longer independent, even if individually strong. Such epistasis can be summarized as resulting from a global non-linearity applied to an underlying linear trait, i.e., as global epistasis. This constraint, in turn, reduces the ruggedness of the sequence-to-function map. By providing a generic mechanistic origin for experimentally observed global epistasis, our work suggests that slow collective physical modes can make biological systems evolvable.

Function in biology arises from the concerted, collective action of individual components. A mutation in any one component can alter the collective state of the system, modulating the effect of later mutations. Multiple mutations can therefore have effects distinct from the sum of their parts. Such epistasis, or non-additivity (Fig. 1a), is found across scales of biological organisation: from individual proteins [1–3], to intracellular genetic [4, 5] and metabolic [6, 7] networks, to complex ecosystems of many species [8, 9]. Apart from being difficult to measure experimentally, epistasis can also hinder the natural evolution of a biological system, by making sequence-to-function maps highly rugged [10], with many local fitness peaks that can trap evolutionary trajectories and thus make evolution more contingent, less predictable, and less reversible [1, 3, 11, 12].

However, recent analyses of deep mutagenesis data [13–15] have suggested that epistasis in some real biological systems may instead be highly constrained. Known as global or non-specific epistasis [1], such epistasis takes the form of a global non-linearity distorting an underlying additive trait. For example, mutations themselves might be effectively additive in determining the folding energy E of a protein, but folding stability, quantified by a non-linear function $f(E)$ of energy (e.g., $f \sim \exp(-E/k_B T)$), will nevertheless show strong epistasis. [14]. In this case, only a few independent numbers – and thus only a few measurements – suffice to specify all other mutational interactions. In addition, the evolutionary consequences of global epistasis are also different: the fitness landscape is expected to be less rugged and easier to navigate [16].

What are the mechanistic determinants of constrained epistasis [3, 14, 17–19]? That is, what kinds of underlying physical interactions or mechanisms give rise to fully rugged, or ‘specific’ [1], epistasis – with accompanying unpredictability and complexity – versus interactions that give rise to a simplified global epistasis instead? One obvious answer is that strong and direct physical interac-

tions give rise to specific epistasis, while non-interacting or weakly interacting sites (e.g., additive contributions to free energy [14]), with a non-linearity introduced elsewhere (e.g., in measurement, or in relating function to fitness [17]), leads to global epistasis. While weak interactions surely lead to global or no epistasis, many cases of interest in biology involve strong physical interactions, as in interactions between residues in the compact core of a protein structure.

Here, we argue that global epistasis can generically arise in biological systems, if their long-time *physical* dynamics – their response to transient perturbations – is described by only a few collective degrees of freedom. These include proteins with a few ‘soft’ mechanical or vibrational modes, as well as gene regulatory networks whose expression levels relax primarily along a few slow collective modes. We show that these systems exhibit a stereotyped response to mutations, with combinations of mutations forced to interact only through the few slow collective physical modes. This, in turn, implies global epistasis, which, in a small perturbation approximation, we diagnose by a reduced rank of the epistatic matrix: that is, the matrix of $\mathcal{O}(N^2)$ pairwise epistatic interactions between N mutations is specified entirely by $\mathcal{O}(N)$ numbers. The corresponding evolutionary fitness landscapes is found to be less rugged and easier to navigate, suggesting that ‘evolvability’ can be selected for by selecting for a separation of biophysical timescales.

Notably, while our arguments rely on testable assumptions about mutations – which we confront with structural data on proteins and proteomic data in *E. coli* – our analysis applies broadly to *any* fitness function in such systems, and might also apply to other non-mutational, high-order interacting systems in biology, such as drug interactions [20–22] or ecological networks [9, 23]. Overall, our results suggest a physical origin for constrained evolutionary epistasis, and rationalizes the occurrence of slow, collective modes in proteins and biological networks.

* amurugan@uchicago.edu

RESULTS

We present our results in terms of distinct models of protein and regulatory network function. In each, we find that if there is a slow dynamical mode (Fig. 1c,d), then mutations only perturb the biological system along a low-dimensional contour in an otherwise high-dimensional configuration space (Fig. 1e,f). As a result, epistasis is global, arising from the non-linearity of fitness along that slow mode.

A. Soft Modes in a Protein Constrain Epistasis

We begin with proteins. The three-dimensional arrangement of atoms in folded proteins forms the physical basis of protein function (i.e. binding to a ligand, or the catalysis of a reaction). A mutation in sequence – i.e. the replacement of one amino acid for another – leads to a deformation in the folded structure (or in an ensemble of folded structures), and a concomitant change in function (e.g. an altered K_d).

Interestingly, many proteins are known to be constrained in their *physical* deformations – i.e., in their response to applied forces due to e.g. ligand binding. Fig. 2a shows an example from a normal mode analysis, which decomposes the physical motions of a protein into a spectrum of orthogonal modes (also known as vibrational modes) [24]. A few ‘soft’ collective motions are found to be of lower energy and thus easier to actuate than other stiffer motions. These collective motions have been extensively studied by molecular dynamics techniques [25], compared against NMR and time-resolved X-ray crystallography [24, 26], and have been proposed as the mechanical basis for protein function, e.g. ligand specificity and allosteric communication [27–31].

Notably, several studies have found that *physical* soft modes constrain *mutation-induced* deformations of a protein to be low dimensional. For e.g., in Fig.2b, we summarize results[32] from a study that compared the variations of protein crystal structure across a protein family, due to mutations, to the geometry of normal modes of single proteins in that family. For 35 different protein families, [32] found that the structural variations across a given family are relatively low-dimensional (4 or 5 dims) and are mostly contained in the subspace spanned by the lowest energy physical modes of any protein in that family. Other studies have performed similar but detailed analyses for particular protein families such as globins[33], the Ras superfamily[34], DHFR [35], HIV-1 protease [36], and T4 lysozyme [37].

We argue that this empirical relationship between *physical* soft modes and *mutation-induced* deformations is to be expected mathematically. Assuming only local physical interactions between residues, we derive the structural deformation $\delta_i \mathbf{r}$, induced by a mutation at residue i , in terms of the physical modes of the protein.

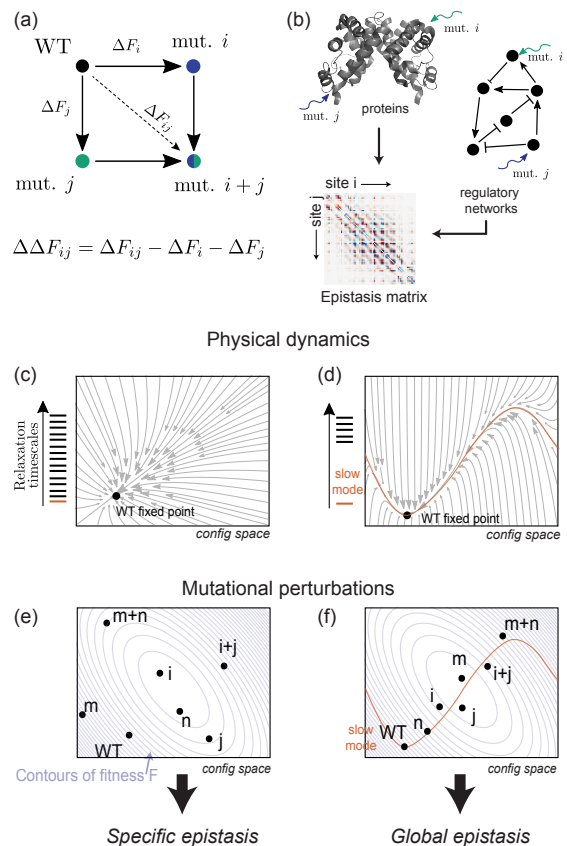


FIG. 1. Slow physical modes can constrain mutational interactions. **a** The non-additivity of two mutations i and j on fitness F defines the epistatic coupling $\Delta \Delta F_{ij}$; **b** epistatic couplings are found at many scales, from within a single protein to across the genome. **c**, **d** We contrast epistasis in systems with qualitatively different *physical* dynamics, e.g., the relaxational dynamics of protein structure or expression levels in a regulatory network. Some biological systems **d** naturally show a large gap in the spectrum of timescales of such relaxation modes; i.e., some relaxation modes (orange) are much slower than others. **e** We argue that without slow modes as in **c**, the effect of mutations is idiosyncratic in the high-dimensional configuration space of the system (e.g. the molecular coordinates of all atoms in a protein). **f** In contrast, with a slow mode as in **d**, we argue that the effect of mutations is mostly confined to the low dimensional subspace (orange) defined by the slow mode. Consequently, while epistatic coupling for each pair (i, j) or (m, n) can still be as strong as in **e**, the couplings are now related to each other through the non-linearity of the fitness function F (purple) along the slow mode (orange), leading to global epistasis.

In the limit of small perturbations, we find (see SI)

$$\delta_i \mathbf{r} \approx \mathcal{H}_0^{-1} \vec{\nabla} \delta_i E(\mathbf{r}_0) \approx \frac{1}{\lambda_0} \left(\hat{\mathbf{v}}_0 \cdot \vec{\nabla} \delta_i E \right) \hat{\mathbf{v}}_0 + \mathcal{O} \left(\frac{1}{\lambda_1} \right) \quad (1)$$

where \mathcal{H}_0 is the Hessian of the wildtype protein’s folding energy about its folded structure \mathbf{r}_0 , $\delta_i E$ is the perturbation in folding energy induced by the mutation. λ_0 and $\hat{\mathbf{v}}_0$ are the energy and geometry of the softest mode;

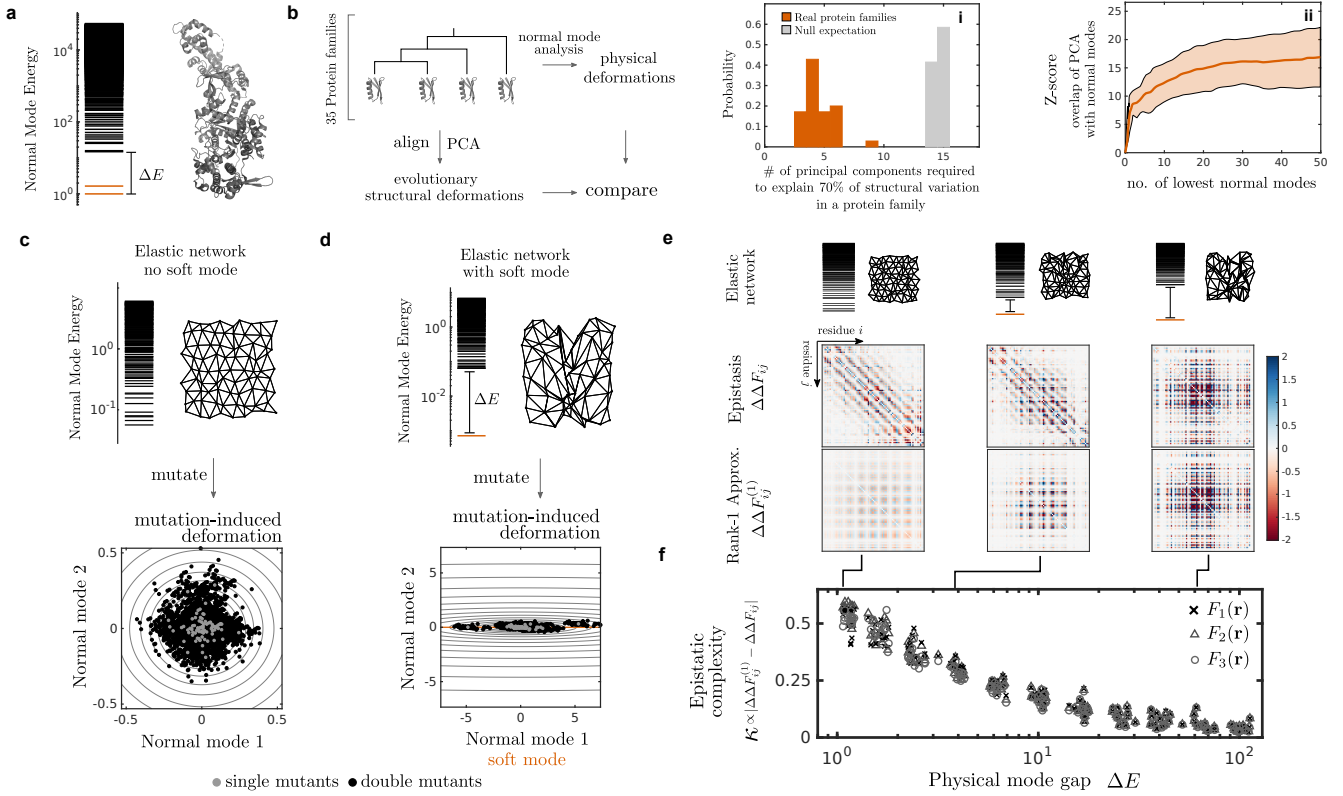


FIG. 2. Soft modes in proteins constrain mutation-induced structural deformations and thus simplify epistasis. **a** Many proteins exhibit one, or a few, soft modes of deformation (orange); quantified by a gap ΔE in their normal mode spectrum (shown for Myosin V, PDB ID: 1W7J). **b** Variations in protein structure across a protein family (due to mutations) are (i) low dimensional (4-5 PCA components); further, (ii) these components have highest overlap with the softest normal modes of a given protein in that family. (PCA components and Z-scores for overlap reproduced from [32]) **c**, **d** Simulated mutation-induced deformations in an elastic network model without (**c**) and with (**d**) a soft mode, shown in the space spanned by the two lowest normal modes; mutations in the background of a soft physical mode deform the protein mostly along that soft mode (energy contours of WT shown in gray). **e** We perform double mutant cycles in a family of ENMs with varying mode gap ΔE (i.e. the ratio of the two lowest normal mode energies), measuring three arbitrarily chosen fitness functions $F(r)$ of structure (symbols, see SI). The resultant epistatic matrices $\Delta\Delta F_{ij}$, and their rank-1 approximations, $\Delta\Delta F_{ij}^{(1)}$, are shown. **f** The epistatic complexity, defined as the median residual $|\Delta\Delta F_{ij}^{(1)} - \Delta\Delta F_{ij}|$, decreases as the physical mode gap ΔE increases.

while λ_1 is the energy of the next softest mode.

That is, in the presence of a soft physical mode, each mutation deforms the protein along that one mode $\hat{\mathbf{v}}_0$, and mutated structures populate a one-dimensional contour in the high-dimensional space of possible structures.

This stereotyping of mutation-induced deformations, Eq. 1, is sufficient to simplify epistasis. Consider a fitness function, F , representing, say, the binding affinity for a ligand, or catalytic efficiency – we place no constraints on the fitness function, supposing only that it can be written as a function of protein structure: $F(\mathbf{r})$. As shown in the SI, in general the epistatic co-efficient between mutations i and j is $\Delta\Delta F_{ij} = (\delta_i \mathbf{r} \cdot \nabla)(\delta_j \mathbf{r} \cdot \nabla)F(r_0)$, which reduces in the presence of a single soft mode to

$$\Delta\Delta F_{ij} \propto \frac{1}{\lambda_0^2} \theta_i \theta_j + c_{ij}, \quad (2)$$

i.e., a rank-1 matrix $\theta_i \theta_j$ (here, $\theta_i = \hat{\mathbf{v}}_0 \cdot \vec{\nabla}_i E$), and a

sparse matrix c_{ij} that is non-zero only for residues i, j in physical contact. Notably, rank-1 matrices are highly constrained, with much fewer independent numbers than a full-rank matrix, and can therefore be reconstructed by fewer measurements. If multiple deformation modes are soft, say k soft modes, the predicted rank of $\Delta\Delta F_{ij}$ is k . Similar observations about epistasis have been made for functions related to protein allostery [28, 38].

Intuitively, this reduction in complexity is due to a dimensional reduction in mutational effects. In principle, the fitness $F(\mathbf{r})$ is a function of all molecular coordinates, and thus can be extremely complex. However, if mutations can sample only a limited set of deformations, as in Eq. 1, the fitness landscape depends only on those few collective coordinates; see Fig. 1d. Mathematically, in the background of a soft mode, the fitness function is simply $F(\{s_i\}) = g(\sum_i \theta_i s_i)$ where $g(\phi)$ is the non-linearity of the fitness function $F(\mathbf{r})$ along the soft mode, $s_i = 0, 1$ is the genotype, and $\sum_i \theta_i s_i$ is

the total mutation-induced deformation along the soft mode. This form, with an overall non-linearity applied to an underlying linear trait, is that of global epistasis [13]. Moreover, expanding any global epistatic function $F(s_i) = g(\sum \theta_i s_i)$ generates strong yet low-rank epistasis of all orders: the 2nd order term is rank-1 (as in Eq. 2) and higher order terms are similarly constrained.

The above result applies for an infinitely large gap ΔE in the normal mode spectrum. We sought to test our results for finite gaps by simulating elastic network models (ENM) of proteins with varying gap ΔE . ENMs have been widely used to analyze ligand binding[39–41] and allostery [27, 28, 30], and are believed to robustly capture the low-frequency motions of many proteins [24, 42]. Introducing mutations in the family of ENMs (see SI for details), we find that mutations in the background of a soft mode result in deformations along that one mode (Fig. 2c,d), confirming Eq. 1. We then performed double-mutant cycles in our simulated networks, measuring epistasis for three arbitrarily chosen fitness functions $F(\mathbf{r})$ detailed in the SI. Fig. 2e presents the epistatic matrix $\Delta\Delta F_{ij}$, compared against a rank-1 approximation.

We find that as the gap ΔE in the *physical* mode spectrum increases, the *epistatic* ‘complexity’ (here, deviation from rank-1) decreases (Fig. 2f), confirming Eq. 2.

B. Slow Modes in Molecular ensembles

An alternative picture of proteins emphasizes the statistical ensemble over a set of discrete configurations $a = 1, \dots, S$; e.g., these configurations could correspond to small structural re-arrangements of the protein, such as broken hydrogen bonds, salt bridges or shifted helices [43]. The WT sequence leads to occupancies $\psi_a^{(\text{WT})}$ of these different states $a = 1, \dots, S$, while mutants can alter the energies of these states and thus result in a different set of occupancies $\psi_a^{(\text{mut.})}$. Fitness $F(\{\psi_a\})$ is determined by these occupancies; such molecular ensembles can generically lead to epistasis [19].

If we perturb the steady state occupancies $\psi_a^{(\text{WT})}$ to $\psi_a^{(\text{pertub.})}$ by some transient physical perturbation (e.g., raising and lowering temperature), $\psi_a^{(\text{pertub.})}$ will relax back to $\psi_a^{(\text{WT})}$ in a way determined by the network of kinetic barriers between states. Such a relaxation process is described by a master equation,

$$\frac{d\psi_a}{dt} = \sum_b M_{ba}\psi_b - \sum_b M_{ab}\psi_a \quad (3)$$

where M_{ab}, M_{ba} are kinetic rates of transition between states a, b . The lowest eigenvalue of M is always zero, reflecting conservation of probability and the corresponding eigenvector gives the steady-state distribution. The next eigenvalue λ_1 and corresponding eigenvector of M determine the slowest relaxation mode in the system. If this mode is much slower than the subsequent modes,

i.e., if $|\lambda_1| \ll |\lambda_p|, p > 1$, then the system is characterized by a slow relaxation mode $\lambda_1, \hat{\mathbf{v}}_1$. For example, such a mode can physically correspond to a meta-stable state (or more generally, a meta-stable ensemble) that generic ensembles quickly relax to; the meta-stable ensemble then slowly relaxes to the steady state distribution.

In the presence of such a slow mode, our earlier analysis follows through. Mutations shift the ensemble in a low-dimensional stereotyped manner. Consequently, epistasis is of the global type and in a perturbative expansion, we find that the 2nd order epistatic term $\Delta\Delta F_{ij}$ is rank-1; see SI for detailed calculations.

C. Slow Modes in Regulatory Networks

Informed by our protein results, we wondered if similar constraints on epistasis may be at play at higher levels of biological organization. In fact, epistasis has been widely investigated at the genomic, metabolic and even ecological levels, often through the lens of the topology of the underlying interaction networks [3–8].

Instead of network topology, we focus here on the underlying dynamics. The dynamics of these biological networks can be characterized by relaxation modes and an accompanying spectrum of timescales (Fig. 3a). For e.g., when a cell is transiently perturbed by changing external conditions (e.g., available nutrients or stressors), the initial perturbation to gene expression levels excites a combination of modes. However, modes with fast relaxation timescales decay rapidly and the response on longer timescales is dominated by the slowest modes.

If a few modes are significantly slower than all other modes, most perturbations will result in shifts in expression levels along the same low dimensional subspace, as measured on longer timescales. Such low dimensionality of expression levels has been reported in proteomics experiments [44, 45] (reproduced in Fig.3c), analyzed in [46–49], and have also been discussed in the context of metabolic regulation of the proteome [50, 51].

Just as a soft mode in a protein stereotypes its response to mutations, a slow manifold in a regulatory network stereotypes its response to mutations or sustained external perturbations. Mathematically, if $\delta_i \mathbf{f}$ represents, say, a change in some regulatory rates due to a mutation i , the shift in steady state expression levels $\delta \mathbf{n}$ may be written as:

$$\delta_i \mathbf{n} \approx \mathcal{J}_0^{-1} \delta_i \mathbf{f} \propto \frac{1}{\lambda_0} \theta_i \hat{\mathbf{v}}_0 + O\left(\frac{1}{\lambda_1}\right) \quad (4)$$

where \mathcal{J}_0 is the Jacobian of the dynamical equations of unperturbed network near its steady state, $\frac{1}{\lambda_0}, \hat{\mathbf{v}}_0$ are the timescale and direction of the slow manifold (computed as eigenvalues and eigenvectors of \mathcal{J}_0), and $\theta_i = \delta_i \mathbf{f} \cdot \hat{\mathbf{v}}_0$. Thus, just as with proteins, mutations in the background of a slow manifold perturb the network along a characteristic direction.

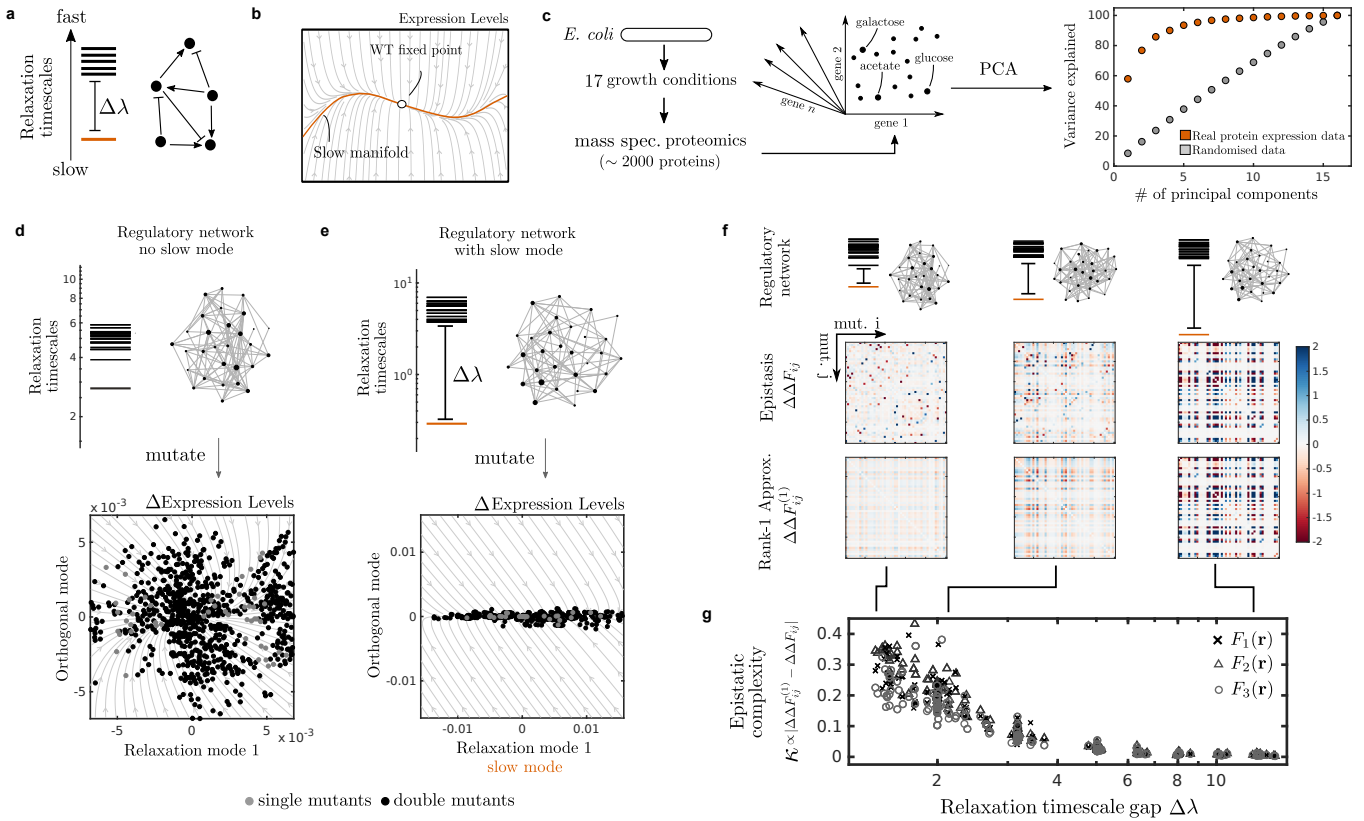


FIG. 3. Slow modes in regulatory networks constrain perturbation of expression levels and simplify epistasis. a Regulatory genetic or metabolic networks exhibit a spectrum of relaxation timescales when perturbed. If a few modes (orange) are significantly slower than others, quantified by a gap $\Delta\lambda$ in the rate spectrum, most perturbations quickly relax to that low dimensional manifold (orange in b) defined by those modes; consequently, expression levels, if measured on longer timescales, are mostly contained within these few slow modes. c Data from [44, 45] suggests that the changes in the *E. coli* proteome (assessed by PCA, orange), measured across 17 different growth conditions, are contained within a low-dimensional manifold (i.e. only 3-4 principal components; gray datapoints obtained by scrambling measured expression levels across growth conditions). d, e We simulate the effect of mutations in a family of regulatory networks (only top 50% of links shown for clarity, node size represents WT expression level) without (d) and with (e) a slow mode, showing changes in expression in the subspace spanned by the lowest mode and an orthogonal direction. In the presence of a slow mode, mutations shift expression levels mostly along the slow mode. f Epistasis $\Delta\Delta F_{ij}$, and its low-rank approximation $\Delta\Delta F_{ij}^{(1)}$, from simulated double mutant cycles in regulatory networks, for three randomly generated fitness functions (see SI). g The epistatic complexity $\kappa \propto |\Delta\Delta F_{ij}^{(0)} - \Delta\Delta F_{ij}^{(1)}|$, reduces as the gap in the relaxation spectrum, $\Delta\lambda$, increases.

Correspondingly, as in Eq. 2 for proteins, we expect that the epistasis is explained by a global non-linearity and, in a small perturbation expansion, the epistatic matrix is low-rank; see SI for derivation.

To test this result, we construct a generic, statistical family of models that are representative of biochemical networks. To be concrete, we consider a family of genetic networks, in which each node represents a gene and edges correspond to, e.g., transcriptional regulation. If n_a is the expression level of gene-product a , the dynamics of the network may be written as:

$$\frac{\partial}{\partial t} n_a = \sum_b k_{ab} \frac{n_b}{n_b + K_{ab}} - \lambda_a n_a \quad (5)$$

where we have chosen Michaelis-Menten kinetic forms for the regulatory terms, with k_{ab} and K_{ab} parameterizing

the regulation $b \rightarrow a$, and λ_a are decay-rates for each gene product due to dilution or degradation. For simplicity, we consider only positive regulation, and suppose that each mutation affects the kinetic parameters k_{ab} and K_{ab} for a particular link $b \rightarrow a$ (see Fig. 3d,e).

We perform simulated double mutant cycles, varying the gap $\Delta\lambda$ in the spectrum of relaxational timescales, and measure fitness $F(\mathbf{n})$ with three randomly generated fitness functions (see SI). We again find that epistatic complexity κ , defined as deviation from rank-1, reduces with an increasing gap $\Delta\lambda$, Figs 3f,g.

Thus, we find that even without tuning the motifs and topology of the network [5, 6], slow collective modes in strongly interacting biological networks lead to constrained, low-rank epistasis.

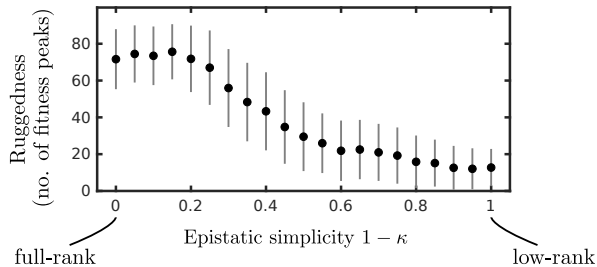


FIG. 4. **Low-rank epistasis makes the sequence-to-function map less rugged.** We simulated adaptive walks on fitness landscapes of varying epistatic complexity, interpolating between low-rank and full-rank epistasis. The number of distinct fitness maxima found, a measure of the ruggedness of the fitness landscape, decreases as epistasis is tuned to be low-rank (error bars show standard deviation over 100 generated fitness landscapes; see SI for details). In conjunction with Figs. 2f, 3f, these results show that slow dynamical modes in proteins and regulatory networks lead to low-rank epistasis and consequently less rugged sequence-to-function maps.

D. Evolutionary consequences

Our work here proposes that slow collective physical modes constrain the epistatic coefficients $\Delta\Delta F_{ij}$ measured in deep mutational screens. Such constrained, or global, epistasis might also affect the ruggedness of sequence-to-function maps and thus have evolutionary consequences [16]. To test this, we considered a family of epistatic matrices $\Delta\Delta F_{ij} = (1 - \kappa)\theta_i\theta_j + \kappa J_{ij}$, parameterising fitness landscapes that interpolate between those with complex epistasis as seen with no physical mode gap (when $\kappa = 1$) and those with simplified epistasis as elicited with a large mode gap (when $\kappa = 0$). Here J_{ij} is a randomly generated full-rank matrix, while $\theta_i\theta_j$ is a random rank-1 matrix.

We simulated adaptive walks on fitness landscapes corresponding to different κ . As shown in Fig. 4, for small κ , adaptive walks discover and get trapped at many more local maxima than for large κ , even though the size of individual epistatic couplings $\Delta\Delta F_{ij}$ are equally large for all κ . See SI for more details.

When combined with Figs. 2f, 3g, our results suggest a striking relationship between *physical* mode gap ΔE , the complexity κ (or equivalently, rank) of the resulting *mutational* epistatic matrix and consequently the ruggedness of *evolutionary* fitness landscapes.

DISCUSSION

We have argued that the physical dynamics of a biological system can easily and generically constrain its epistatic complexity. We considered proteins and regulatory networks whose response to perturbations is dominated by a few slow collective modes on longer timescales.

We argued, with support from analyses of existing data sets, that such slow collective modes can effectively limit accessible deformations to a low dimensional subspace of a high-dimensional configuration space (e.g., atomic structure or ensemble occupancies for proteins, expression levels for gene regulatory networks). Correspondingly, epistasis is predicted to be global (i.e., a global non-linearity applied to an underlying linear trait) and the pairwise epistatic matrix is predicted to be low rank.

Our theory relies on experimentally testable assumptions about mutation-induced deformations and their relationship with physical modes. For instance, a conservative estimate of the mode gap required to give global epistasis gives a scaling with system size N as \sqrt{N} . For a protein with ~ 100 amino acids or a regulatory network with a 100 genes, this requires a mode-gap of $\lambda_1/\lambda_0 \approx 10$. This is in line with estimates for mode gaps in real proteins [52]. We also presented evidence from the literature for how such slow modes constrain mutational-deformations in proteins, which typically compare experimentally determined mutation-induced structural deformations to computed normal modes [33, 37], and generally find a non-trivial overlap between the two [32].

A deeper test of our ideas requires a detailed experimental comparison between physical and mutational experiments. For instance, in proteins a direct experimental characterization of soft modes is to be compared against measured epistasis via deep mutational scans. Data of both types are currently coming online. Deep mutational scans have been performed for a few proteins [53–55] (and in fact, shown to be consistent with global epistasis [13]). Meanwhile, electric-field stimulated X-ray (EFX) experiments have directly probed the soft modes of a protein, by applying an electric field and capturing the deformations of a protein by time-resolved X-ray crystallography on the 100 ns timescale [26]. Similarly, in the context of gene regulation, one should correlate the effects of mutagenesis with physiological perturbations such as nutrient shifts [44, 51], as well as with measurements of genetic epistasis.

Notably, while our results rely on the nature of mutation-induced deformations, we make few assumptions about the fitness function itself; any fitness function of coordinates in which a slow mode dominates is predicted to show global epistasis. Further, we showed that the relevant slow modes can exist in diverse spaces - structure (quantified by normal mode energies), statistical ensembles (eigenvalues of a master equation) or non-linear regulatory networks (Lyapunov exponents). Note that the latter two systems may not have any equilibrium energy function, with Lyapunov exponents playing the role of normal mode energies.

More broadly, our work highlights the need to understand the connection between the underlying dynamics of a system and its observed epistasis [19, 56]. Traditionally, strong specific epistasis is often interpreted as evidence of direct interaction, and global epistasis seen as the result of weak or no interactions (e.g., due to ad-

ditive contributions to free energy) [15]. Our work shows that, counterintuitively, global epistasis can also result from strong interactions, if the interactions result in a collective slow mode.

In conclusion, we have analyzed the evolutionary consequences of a biophysical slow mode. Such slow modes are often linked to particular functions, such as allostery in proteins [29] or metabolic control of gene expression [51]. Our work suggests an alternative benefit of such slow modes, namely evolvability. This suggests that per-

haps slow modes might have evolved for evolvability first, and only later been repurposed for other functions.

Acknowledgements We are grateful to Rama Ranganathan, Sidney Nagel, Tobin Sosnick, Joseph Thornton, Weerapat Pittayakanchit, Yaakov Kleorin, and Lauren McGough, as well as the Ranganathan and Murugan groups, for helpful discussions, and to Tyler Starr and Jakub Otwinowski for feedback. KH thanks the James S. McDonnell Foundation for support via a postdoctoral fellowship. AM acknowledge support from the Simons Investigator program.

-
- [1] Tyler N. Starr and Joseph W. Thornton. Epistasis in protein evolution. *Protein Science*, 25(7):1204–1218, jul 2016.
- [2] Rhys M. Adams, Justin B. Kinney, Aleksandra M. Walczak, and Thierry Mora. Epistasis in a Fitness Landscape Defined by Antibody-Antigen Binding Free Energy. *Cell Systems*, 8(1):86–93.e3, jan 2019.
- [3] Júlia Domingo, Pablo Baeza-Centurion, and Ben Lehner. The Causes and Consequences of Genetic Interactions (Epistasis). *Annual Review of Genomics and Human Genetics*, 20(1):annurev-genom-083118-014857, aug 2019.
- [4] Javier Macía, Ricard V. Solé, and Santiago F. Elena. The causes of epistasis in genetic networks. *Evolution*, 66(2):586–596, feb 2012.
- [5] José I. Rojas Echenique, Sergey Kryazhimskiy, Alex N. Nguyen Ba, and Michael M. Desai. Modular epistasis and the compensatory evolution of gene deletion mutants. *PLoS Genetics*, 15(2):e1007958, feb 2019.
- [6] Daniel Segrè, Alexander DeLuna, George M. Church, and Roy Kishony. Modular epistasis in yeast metabolism. *Nature Genetics*, 37(1):77–83, jan 2005.
- [7] Djordje Bajić, Jean C.C. Vila, Zachary D Blount, and Alvaro Sánchez. On the deformability of an empirical fitness landscape by microbial evolution. *Proceedings of the National Academy of Sciences of the United States of America*, 115(44):11286–11291, oct 2018.
- [8] Alison L Gould, Vivian Zhang, Lisa Lamberti, Eric W Jones, Benjamin Obadia, Nikolaos Korasidis, Alex Gavryushkin, Jean M Carlson, Niko Beerenwinkel, and William B Ludington. Microbiome interactions shape host fitness. *Proceedings of the National Academy of Sciences of the United States of America*, 115(51):E11951–E11960, dec 2018.
- [9] Jacopo Grilli, György Barabás, Matthew J. Michalska-Smith, and Stefano Allesina. Higher-order interactions stabilize dynamics in competitive network models. *Nature*, 548(7666):210–213, aug 2017.
- [10] Stuart A. Kauffman and Edward D. Weinberger. The NK model of rugged fitness landscapes and its application to maturation of the immune response. *Journal of Theoretical Biology*, 141(2):211–245, 1989.
- [11] Tyler N. Starr, Lora K. Picton, and Joseph W. Thornton. Alternative evolutionary histories in the sequence space of an ancient protein. *Nature*, 549(7672):409–413, sep 2017.
- [12] Tyler N. Starr, Julia M. Flynn, Parul Mishra, Daniel N.A. Bolon, and Joseph W. Thornton. Pervasive contingency and entrenchment in a billion years of Hsp90 evolution. *Proceedings of the National Academy of Sciences of the United States of America*, 115(17):4453–4458, apr 2018.
- [13] Jakub Otwinowski, David M. McCandlish, and Joshua B. Plotkin. Inferring the shape of global epistasis. *Proceedings of the National Academy of Sciences of the United States of America*, 115(32):E7550–E7558, 2018.
- [14] Jakub Otwinowski. Biophysical inference of epistasis and the effects of mutations on protein stability and function. *Molecular Biology and Evolution*, 35(10):2345–2354, aug 2018.
- [15] Zachary R Sailer and Michael J Harms. Uninterpretable interactions: epistasis as uncertainty. *bioRxiv*, page 378489, 2018.
- [16] Sergey Kryazhimskiy, Daniel P. Rice, Elizabeth R. Jerison, and Michael M. Desai. Global epistasis makes adaptation predictable despite sequence-level stochasticity. *Science*, 344(6191):1519–1522, jun 2014.
- [17] Ben Lehner. Molecular mechanisms of epistasis within and between genes. *Trends in Genetics*, 27(8):323–331, aug 2011.
- [18] Mark A. DePristo, Daniel M. Weinreich, and Daniel L. Hartl. Missense meanderings in sequence space: A biophysical view of protein evolution. *Nature Reviews Genetics*, 6(9):678–687, sep 2005.
- [19] Zachary R. Sailer and Michael J. Harms. Molecular ensembles make evolution unpredictable. *Proceedings of the National Academy of Sciences of the United States of America*, 114(45):11938–11943, 2017.
- [20] Pamela Yeh, Ariane I Tschumi, and Roy Kishony. Functional classification of drugs by properties of their pairwise interactions. *Nature Genetics*, 38(4):489–494, apr 2006.
- [21] Remy Chait, Allison Craney, and Roy Kishony. Antibiotic interactions that select against resistance. *Nature*, 446(7136):668–671, apr 2007.
- [22] Kevin Wood, Satoshi Nishida, Eduardo D. Sontag, and Philippe Cluzel. Mechanism-independent method for predicting response to multidrug combinations in bacteria. *Proceedings of the National Academy of Sciences of the United States of America*, 109(30):12254–12259, jul 2012.
- [23] Alicia Sanchez-Gorostiaga, Djordje Bajić, Melisa L. Osborne, Juan F Poyatos, and Alvaro Sanchez. High-order interactions dominate the functional landscape of microbial consortia. *bioRxiv*, page 333534, may 2018.
- [24] Ivet Bahar, Timothy R. Lezon, Ahmet Bakan, and In-

- dira H. Shrivastava. Normal mode analysis of biomolecular structures: Functional mechanisms of membrane proteins. *Chemical Reviews*, 110(3):1463–1497, 2010.
- [25] B. Brooks and M. Karplus. Harmonic dynamics of proteins: Normal modes and fluctuations in bovine pancreatic trypsin inhibitor. *Proceedings of the National Academy of Sciences of the United States of America*, 80(21 I):6571–6575, nov 1983.
- [26] Doeke R. Hekstra, K. Ian White, Michael A. Socolich, Robert W. Henning, Vukica Šrajter, and Rama Ranganathan. Electric-field-stimulated protein mechanics. *Nature*, 540(7633):400–405, dec 2016.
- [27] Jason W. Rocks, Nidhi Pashine, Irmgard Bischofberger, Carl P. Goodrich, Andrea J. Liu, and Sidney R. Nagel. Designing allostery-inspired response in mechanical networks. *Proceedings of the National Academy of Sciences of the United States of America*, 114(10):2520–2525, mar 2017.
- [28] Sandipan Dutta, Jean Pierre Eckmann, Albert Libchaber, and Tsvi Tlusty. Green function of correlated genes in a minimal mechanical model of protein evolution. *Proceedings of the National Academy of Sciences of the United States of America*, 115(20):E4559–E4568, 2018.
- [29] Shoshana J. Wodak, Emanuele Paci, Nikolay V. Dokholyan, Igor N. Berezovsky, Amnon Horovitz, Jing Li, Vincent J. Hilser, Ivet Bahar, John Karanicolas, Gerhard Stock, Peter Hamm, Roland H. Stote, Jerome Eberhardt, Yasmine Chebaro, Annick Dejaegere, Marco Cecchini, Jean Pierre Changeux, Peter G. Bolhuis, Jocelyne Vreede, Pietro Faccioli, Simone Orioli, Riccardo Ravaasio, Le Yan, Carolina Brito, Matthieu Wyart, Paraskevi Gkeka, Ivan Rivalta, Giulia Palermo, J. Andrew McCammon, Joanna Panecka-Hofman, Rebecca C. Wade, Antonella Di Pizio, Masha Y. Niv, Ruth Nussinov, Chung Jung Tsai, Hyunbum Jang, Dmzmitry Padhorny, Dima Kozakov, and Tom McLeish. Allostery in Its Many Disguises: From Theory to Applications. *Structure*, 27(4):566–578, apr 2019.
- [30] Le Yan, Riccardo Ravaasio, Carolina Brito, and Matthieu Wyart. Architecture and coevolution of allosteric materials. *Proceedings of the National Academy of Sciences of the United States of America*, 114(10):2526–2531, mar 2017.
- [31] Olivier Rivoire. Parsimonious evolutionary scenario for the origin of allostery and coevolution patterns in proteins. *Physical Review E*, 100(3):032411, sep 2019.
- [32] Alejandra Leo-Macias, Pedro Lopez-Romero, Dmitry Lupyman, Daniel Zerbino, and Angel R. Ortiz. An analysis of core deformations in protein superfamilies. *Biophysical Journal*, 88(2):1291–1299, feb 2005.
- [33] Julián Echave and Francisco M. Fernández. A perturbative view of protein structural variation. *Proteins: Structure, Function and Bioinformatics*, 78(1):173–180, jan 2010.
- [34] Francesco Raimondi, Modesto Orozco, and Francesca Fanelli. Deciphering the Deformation Modes Associated with Function Retention and Specialization in Members of the Ras Superfamily. *Structure*, 18(3):402–414, mar 2010.
- [35] Thomas H. Rod, Jennifer L. Radkiewicz, and Charles L. Brooks. Correlated motion and the effect of distal mutations in dihydrofolate reductase. *Proceedings of the National Academy of Sciences of the United States of America*, 100(12):6980–6985, jun 2003.
- [36] Lei Yang, Guang Song, Alicia Carriquiry, and Robert L. Jernigan. Close Correspondence between the Motions from Principal Component Analysis of Multiple HIV-1 Protease Structures and Elastic Network Modes. *Structure*, 16(2):321–330, feb 2008.
- [37] Neeti Sinha and Ruth Nussinov. Point mutations and sequence variability in proteins: Redistributions of preexisting populations. *Proceedings of the National Academy of Sciences of the United States of America*, 98(6):3139–3144, mar 2001.
- [38] Jean-Pierre Eckmann, Jacques Rougemont, and Tsvi Tlusty. Colloquium : Proteins: The physics of amorphous evolving matter . *Reviews of Modern Physics*, 91(3):031001, jul 2019.
- [39] Dror Tobi and Ivet Bahar. Structural changes involved in protein binding correlate with intrinsic motions of proteins in the unbound state. *Proceedings of the National Academy of Sciences of the United States of America*, 102(52):18908–18913, 2005.
- [40] Ahmet Bakan and Ivet Bahar. The intrinsic dynamics of enzymes plays a dominant role in determining the structural changes induced upon inhibitor binding. *Proceedings of the National Academy of Sciences of the United States of America*, 106(34):14349–14354, 2009.
- [41] Shou-Wen Wang, Anne-Florence Bitbol, and Ned S. Wingreen. Revealing evolutionary constraints on proteins through sequence analysis. *PLOS Computational Biology*, 15(4):e1007010, apr 2019.
- [42] Monique M. Tirion. Large amplitude elastic motions in proteins from a single-parameter, atomic analysis. *Physical Review Letters*, 77(9):1905–1908, aug 1996.
- [43] Robert B. Best, Kresten Lindorff-Larsen, Mark A. DePristo, and Michele Vendruscolo. Relation between native ensembles and experimental structures of proteins. *Proceedings of the National Academy of Sciences of the United States of America*, 103(29):10901–10906, jul 2006.
- [44] Alexander Schmidt, Karl Kochanowski, Silke Vedeelaar, Erik Ahrné, Benjamin Volkmer, Luciano Callipo, Kévin Knoops, Manuel Bauer, Ruedi Aebersold, and Matthias Heinemann. The quantitative and condition-dependent Escherichia coli proteome. *Nature Biotechnology*, 34(1):104–110, jan 2016.
- [45] Uri Barenholz, Leeat Keren, Eran Segal, and Ron Milo. A minimalistic resource allocation model to explain ubiquitous increase in protein expression with growth rate. *PLoS ONE*, 11(4):e0153344, apr 2016.
- [46] Kunihiko Kaneko, Chikara Furusawa, and Tetsuya Yomo. Universal relationship in gene-expression changes for cells in steady-growth state. *Physical Review X*, 5(1), 2015.
- [47] Chikara Furusawa and Kunihiko Kaneko. Formation of dominant mode by evolution in biological systems. *Physical Review E*, 97(4):42410, 2018.
- [48] Kunihiko Kaneko and Chikara Furusawa. Macroscopic Theory for Evolving Biological Systems Akin to Thermodynamics. *Annual Review of Biophysics*, 47(1):273–290, may 2018.
- [49] Takuya U. Sato and Kunihiko Kaneko. Evolutionary dimension reduction in phenotypic space. 2019.
- [50] Conghui You, Hiroyuki Okano, Sheng Hui, Zhongge Zhang, Minsu Kim, Carl W. Gunderson, Yi-Ping Wang, Peter Lenz, Dalai Yan, and Terence Hwa. Coordination of bacterial proteome with metabolism by cyclic AMP signalling. *Nature*, 500(7462):301–306, aug 2013.

- [51] David W. Erickson, Severin J. Schink, Vadim Patsalo, James R. Williamson, Ulrich Gerland, and Terence Hwa. A global resource allocation strategy governs growth transition kinetics of *Escherichia coli*. *Nature*, 551(7678):119–123, nov 2017.
- [52] Yuichi Togashi and Alexander S Mikhailov. Nonlinear relaxation dynamics in elastic networks and design principles of molecular machines. *Proceedings of the National Academy of Sciences of the United States of America*, 104(21):8697–702, may 2007.
- [53] C. Anders Olson, Nicholas C. Wu, and Ren Sun. A comprehensive biophysical description of pairwise epistasis throughout an entire protein domain. *Current Biology*, 24(22):2643–2651, nov 2014.
- [54] Victor H Salinas and Rama Ranganathan. Coevolution-based inference of amino acid interactions underlying protein function. *eLife*, 7, jul 2018.
- [55] Guillaume Diss and Ben Lehner. The genetic landscape of a physical interaction. *eLife*, 7, 2018.
- [56] Griffin Chure, Manuel Razo-Mejia, Nathan M. Belliveau, Tal Einav, Zofii A. Kaczmarek, Stephanie L. Barnes, Mitchell Lewis, and Rob Phillips. Predictive shifts in free energy couple mutations to their phenotypic consequences. *Proceedings of the National Academy of Sciences*, 116(37):18275–18284, sep 2019.

Physical constraints on epistasis

SI

K. Husain, A. Murugan

Department of Physics, the University of Chicago

CONTENTS

I. Global and low-rank epistasis in proteins with a soft mechanical mode	1
A. Theory	1
Mutation-induced deformations	2
Global epistasis	3
Low-rank epistasis	3
How big a gap?	4
B. Simulation	4
Model	4
Obtaining a soft mode: Monte Carlo algorithm	5
Mutations in the ENM	5
Fitness functions, double-mutant cycles, and analysis of epistatic matrix	6
C. ENM-derived normal mode analysis of PDB structures	6
D. Relating evolutionary and physical deformations	6
II. Global and low-rank epistasis in protein ensembles	7
A. Theory	7
III. Global and low-rank epistasis in regulatory networks with a slow manifold	8
A. Theory	8
B. Numerical methods	9
Model	9
Varying the gap in the Lyapunov spectrum	9
Mutations, fitness, and epistasis	9
C. Principal component analysis of <i>E. coli</i> proteomics data	10
IV. Low-rank epistasis and evolutionary ruggedness	10
References	10

I. GLOBAL AND LOW-RANK EPISTASIS IN PROTEINS WITH A SOFT MECHANICAL MODE

A. Theory

We begin, as in the main text, with proteins. Our goal is to relate the epistatic co-efficient, $\Delta\Delta F_{ij}$, of some (arbitrary) function (e.g. binding affinity for a ligand) to the mechanical modes of the protein. Recall the sequence-to-function map of the protein

$$\text{sequence } \mathbf{s} \rightarrow \text{function } F(\mathbf{s}) \quad (1)$$

from which we define epistasis in the usual single reference manner, as an expansion of the fitness function $F(\mathbf{s})$ around the wildtype genotype (here, \mathbf{s} is a binary vector representation of the genotype, where $s_i = 1$ if residue i is mutated and 0 otherwise):

$$F(\mathbf{s}) \equiv F(\mathbf{r}(\mathbf{s})) = \underbrace{F_0}_{\text{WT fitness}} + \sum_i \Delta F_i s_i + \sum_{i>j} \Delta\Delta F_{ij} s_i s_j + \sum_{i>j>k} \Delta\Delta\Delta F_{ijk} s_i s_j s_k + \dots \quad (2)$$

Key to the calculation is to express the function of the protein (e.g., its binding affinity or enzymatic activity), F , in terms of its physical structure, schematically denoted \mathbf{r} (we shall more precisely define \mathbf{r} in a moment): $F(\mathbf{r})$. The sequence-to-function map then conceptually decomposes into two steps: sequence to structure, and structure to function:

$$\text{sequence } \mathbf{s} \rightarrow \text{structure } \mathbf{r}(\mathbf{s}) \rightarrow \text{function } F(\mathbf{r}(\mathbf{s}))$$

Before proceeding, we note that the function of the protein may additionally depend on sequence directly, i.e. not through the structure \mathbf{r} , $F(\mathbf{r}(\mathbf{s}), \mathbf{s})$. For instance, the precise chemical identity of the amino acid at a particular site may be crucial – however, it is difficult to imagine that this is true outside of the small number of residues that form the protein’s active site. Thus, for the remainder of the paper, we neglect this potential direct dependence.

Mutation-induced deformations

First, we compute the structural deformation induced by mutations in a protein, in a small perturbation approximation. Represent the structure of the protein by a single vector \mathbf{r} – containing, say, the concatenated spatial positions of all N atoms in the structure. In the absence of external forcing, the structure relaxes in the folding energy $E(\mathbf{r})$:

$$\frac{\partial}{\partial t} \mathbf{r} = -\nabla E(\mathbf{r}) \quad (3)$$

The sequence specifies the form of the energy E – we shall discuss this dependence in a moment, but first let us denote the wildtype energy by E_0 . The wildtype structure \mathbf{r}_0 is found at the minimum of $E_0(\mathbf{r})$, satisfying:

$$-\nabla E_0(\mathbf{r}_0) = 0 \quad (4)$$

Consider now a mutation (or multiple mutations), which perturbs the folding energy function $E(\mathbf{r})$. We compute the resultant deformation in structure. This is easily done if we use a book-keeping parameter ϵ . Denote the modified energy function by $E(\mathbf{r}) = E_0(\mathbf{r}) + \epsilon \delta E(\mathbf{r})$. We look for a new minimum perturbatively in ϵ : $\mathbf{r} = \mathbf{r}_0 + \epsilon \delta \mathbf{r} + \dots$. Expanding Eq. 3 to first order in ϵ at steady state:

$$\begin{aligned} 0 &= -\nabla E_0(\mathbf{r}_0 + \epsilon \delta \mathbf{r} + \dots) - \epsilon \nabla \delta E(\mathbf{r}_0 + \epsilon \delta \mathbf{r} + \dots) \\ &\approx -\nabla E_0(\mathbf{r}_0) - \epsilon (\mathcal{H}_0 \delta \mathbf{r} + \nabla \delta E(\mathbf{r}_0)) \end{aligned} \quad (5)$$

where the matrix \mathcal{H}_0 is the Hessian of the wildtype energy $E_0(\mathbf{r})$ evaluated at the wildtype structure \mathbf{r}_0 . The first term is identically 0, and so we obtain for the mutation-induced deformation:

$$\delta \mathbf{r} = -\mathcal{H}_0^{-1} \nabla \delta E(\mathbf{r}_0) \quad (6)$$

where the inverse \mathcal{H}_0^{-1} is to be understood in the Morse-Penrose sense (i.e. projecting out the trivial zero-modes corresponding to global rotations and translations).

Now let us suppose that the wildtype protein has a single soft mode. Mathematically, this corresponds to an eigenvector of \mathcal{H}_0 , \hat{v}_0 , with an eigenvalue λ_0 much smaller than any other eigenvalue λ_m , $m \neq 0$. Expanding \mathcal{H}_0^{-1} in the eigenbasis and keeping only the largest term (which corresponds to the eigenmode \hat{v}_0):

$$\begin{aligned} \delta \mathbf{r} &= -\left(\frac{1}{\lambda_0} \hat{v}_0 \hat{v}_0^T + \dots \right) \nabla \delta E \\ &= -\sum_{m=0}^{3N-7} \frac{1}{\lambda_m} \hat{v}_m (\hat{v}_m \cdot \nabla \delta E) \\ &\approx \frac{1}{\lambda_0} \hat{v}_0 \underbrace{(-\hat{v}_0 \cdot \nabla \delta E)}_{\phi} \end{aligned} \quad (7)$$

where we have defined the deformation magnitude along the soft mode, ϕ . Thus, as advertised in the main text, mutations in the background of the soft mode deform the protein preferentially along that mode, with a magnitude given by ϕ .

Global epistasis

To proceed, we need to discuss how the deformation magnitude ϕ depends on the number of mutations made. For concreteness, let us introduce the binary variable $s_i = 0$ (1) when residue i is wildtype (mutant). The vector \mathbf{s} , with elements s_i , thus represents the sequence of the protein. If we suppose that the energy function $E(\mathbf{r})$ is a sum of pairwise terms between atoms, then the most general form for the perturbed energy function δE is

$$\delta E = \sum_i \delta_i E s_i + \sum_{i>j} \delta_{ij} E s_i s_j \quad (8)$$

where $\delta_i E$ is the change in energy due to the mutation i alone, and $\delta_{ij} E$ is the contribution of the double mutant i and j . Notably, $\delta_{ij} E$ will only be non-zero only when residues i and j are directly interacting physically. As we suppose that physical interactions are local, $\delta_{ij} E$ is thus non-zero only when i and j are in contact – that is, the matrix $\delta_{ij} E$ is sparse and has the structure of the contact matrix of the protein.

Inserting the expression for δE into Eq. 7:

$$\phi = \sum_i \underbrace{-\hat{v}_0 \cdot \nabla \delta_i E}_{\theta_i} s_i + \sum_{i>j} \underbrace{-\hat{v}_0 \cdot \nabla \delta_{ij} E}_{C_{ij}} s_i s_j \quad (9)$$

which serves as a definition of θ_i and C_{ij} . Note that the deformation magnitude ϕ is nearly additive in mutations – differing only by a sparse second-order term induced by physical contacts.

Now consider a fitness function for the protein (representing, for instance, the binding affinity of the protein for a ligand, or the catalytic rate of an enzymatic reaction). In general, this quantitative trait is a function of both protein structure and sequence: $F(\mathbf{r}, \mathbf{s})$. Let us assume, however, the direct dependence on sequence is negligible: likely involving only residues directly at the active site of the protein. We thus write it as only a function of structure $F(\mathbf{r})$.

The fitness of a mutated sequence, with sequence \mathbf{s} and structure $\mathbf{r}_0 + \delta \mathbf{r}$ is $F(\mathbf{r}_0 + \delta \mathbf{r}(\mathbf{s}))$. We use Eqs. 7 and 9 to rewrite the fitness in terms of the scalar variable ϕ :

$$\begin{aligned} g(\phi) &\equiv F\left(\mathbf{r}_0 + \frac{\hat{v}_0}{\lambda_0} \phi\right) \\ \phi(\mathbf{s}) &= \sum_i \theta_i s_i + \sum_{i>j} C_{ij} s_i s_j \end{aligned} \quad (10)$$

which, except for the sparse matrix C_{ij} , is in the standard form for global epistasis, as defined in, e.g., [1].

Low-rank epistasis

Let us further suppose that ϕ is small and we can Taylor expand $g(\phi)$ to second order. Grouping terms by the order of mutations (i.e. s_i):

$$g(\phi) \approx g(0) + \sum_i (g'(0) + g''(0) \theta_i) \theta_i s_i + \sum_{i>j} g''(0) (\theta_i \theta_j + c_{ij}) s_i s_j \quad (11)$$

where c_{ij} are terms that involve C_{ij} and correspondingly have the structure of the contact matrix.

By comparison with the standard form of an epistatic expansion:

$$F(s_i) = F_0 + \sum \Delta F_i s_i + \sum \Delta \Delta F_{ij} s_i s_j + \dots \quad (12)$$

we arrive at the low-rank form of epistasis advertised in the main text:

$$\Delta \Delta F_{ij} \propto \theta_i \theta_j + c_{ij} \quad (13)$$

A slightly different derivation of Eq. 13 is instructive. For simplicity, let us neglect the contact term in Eq. 8, writing the structural deformation as a function of sequence as:

$$\delta \mathbf{r}(\mathbf{s}) = \sum_i \delta_i \mathbf{r} s_i \quad (14)$$

Then,

$$F(\mathbf{r}_0 + \delta\mathbf{r}) \approx F(\mathbf{r}_0) + \sum_i (\delta\mathbf{r}_i \cdot \nabla) F(\mathbf{r}_0) s_i + \frac{1}{2} \sum_{i,j} (\delta\mathbf{r}_i \cdot \nabla) (\delta\mathbf{r}_j \cdot \nabla) F(\mathbf{r}_0) s_i s_j \quad (15)$$

Notice that we have not yet invoked the existence of a soft mode. In bracket notation, the co-efficient of $s_i s_j$ – the epistatic co-efficient – is $\langle \delta_i \mathbf{r} | \nabla^2 F | \delta_j \mathbf{r} \rangle$, where the matrix $\nabla^2 F$ is the Hessian of the fitness function, evaluated at \mathbf{r}_0 . Expanding $\delta_i \mathbf{r}$ in terms of the WT modes \hat{v}_m :

$$\begin{aligned} \Delta\Delta F_{ij} &\sim \langle \delta_i \mathbf{r} | \nabla^2 F | \delta_j \mathbf{r} \rangle \\ &= \sum_{m=0}^{3N-7} \frac{1}{\lambda_m^2} \langle \hat{v}_m | \nabla^2 F | \hat{v}_m \rangle \langle \hat{v}_m | \nabla \delta_i E \rangle \langle \hat{v}_m | \nabla \delta_j E \rangle \\ &\approx \frac{1}{\lambda_0^2} \langle \hat{v}_0 | \nabla^2 F | \hat{v}_0 \rangle \theta_i \theta_j + \mathcal{O}\left(\frac{1}{\lambda_1^2}\right) \end{aligned} \quad (16)$$

where the final simplification holds only when there is a sufficiently (see next section) soft mode. The expression above makes clear that without a soft mode, each $\Delta\Delta F_{ij}$ is a different matrix element of the matrix $\nabla^2 F$, and is thus an arbitrary number that depends on the idiosyncratic deformations $\delta_i \mathbf{r}$, $\delta_j \mathbf{r}$. With a soft mode, however, the matrix element reduces to a const. \times the product of scalars, $\theta_i \theta_j$ – and thus the epistatic matrix $\Delta\Delta F_{ij}$ is rank 1.

How big a gap?

How large a gap in the normal mode spectrum is required to obtain global epistasis? Consider Eq. 7,

$$\delta\mathbf{r} = \frac{1}{\lambda_0} \hat{v}_0 (\hat{v}_0 \cdot \mathbf{g}) + \sum_{m=1}^{M-1} \frac{1}{\lambda_m} \hat{v}_m (\hat{v}_m \cdot \mathbf{g}) \quad (17)$$

where we have defined the mutation-induced force $\mathbf{g} \equiv -\nabla \delta E$, and use M to represent the number of modes ($M = 3N - 6$ for N atoms in 3D).

As argued above, global epistasis arises when the deformation $\delta\mathbf{r}$ is along the soft mode \hat{v}_0 for an arbitrary mutation-induced force \mathbf{g} . That is, the projection of $\delta\mathbf{r}$ onto \hat{v}_0 is of much greater magnitude than the projection orthogonal to \hat{v}_0 :

$$\frac{1}{\lambda_0^2} (\hat{v}_0 \cdot \mathbf{g})^2 \gg \sum_{m=1}^{M-1} \frac{1}{\lambda_m^2} (\hat{v}_m \cdot \mathbf{g})^2 \quad (18)$$

We compute the required mode-gap in the following manner. Let us suppose that all λ_m , $m > 0$, are of similar magnitude $\lambda_1 > \lambda_0$. As we are interested in a typical mutation-induced force \mathbf{g} , we estimate $\hat{v}_m \cdot \mathbf{g}$ by the average magnitude of two random vectors in a space of dimension dN (where d is the spatial dimension and N is the number of atoms), denoted by α :

$$\frac{1}{\lambda_0^2} \alpha^2 \gg (M-1) \frac{1}{\lambda_1^2} \alpha^2 \quad (19)$$

Rearranging, we arrive at:

$$\Delta E \equiv \frac{\lambda_1}{\lambda_0} \gg \sqrt{M-1} \quad (20)$$

As the number of modes M grows linearly with the number of components of the system, N , we arrive at the \sqrt{N} scaling advertised in the main text.

B. Simulation

Model

To mimic protein mechanics, we follow in the footsteps of recent work [2–4] and simulate a 2D arrangement of nodes and springs (a so-called ‘elastic network model’ or ENM), where nodes represent, e.g., the C- α atoms of each

residue. Indexing nodes by i , the energy is:

$$E = \frac{1}{2} \sum_{i>j} k_{ij} (|\mathbf{r}_i - \mathbf{r}_j| - l_{ij})^2 \quad (21)$$

where the spring constant $k_{ij} = k$ if i, j are in contact and 0 otherwise, and l_{ij} is the rest-length of the spring between i and j . We choose $k = 1$, and set the rest length l_{ij} by the distance between i and j in the wildtype structure \mathbf{r}_0 (that is, the wildtype is unstrained).

All spring networks are initialised with a slightly perturbed hexagonal lattice, of size 9×9 nodes, with each node connected by springs to its nearest neighbours. All springs are initialised with rest lengths such that the network, in its resting configuration, is unstressed. Units of length are set by the average distance between a node and its nearest neighbour. We treat all deformations in the linear approximation, as is commonly done with elastic network models of protein mechanics [2, 3, 5].

Obtaining a soft mode: Monte Carlo algorithm

We engineer in a soft mode by a simple Monte Carlo algorithm. Briefly, at each step the algorithm selects a node and displaces it by a small amount $\delta\mathbf{x}$, each of whose components is picked uniformly from the interval $[-0.025, 0.025]$. The rest lengths of all springs connected to the node are recomputed so that the structure remains unstressed. The Hessian of the network is computed and diagonalised, and the ratio of the two lowest modes is computed,

$$\Delta E \equiv \frac{\lambda_1}{\lambda_0} \quad (22)$$

after excluding the 3 modes corresponding to global translations and rotations, that have eigenvalue 0. The move is accepted if two criteria are met:

1. ΔE increases
2. The inverse participation ratio of the softest mode \hat{v}_0 , defined as $\sum (v_0)_i^4 / \sum (v_0)_i^2$, decreases, or is already below a set threshold (here taken to be $2/N$, where $N = 9 \times 9 = 81$ is the number of nodes). This is to prevent the formation of a localised soft mode, as opposed to the desired collective motion.

If these criteria are met, the move is accepted; otherwise, it is rejected. The process continues until the desired value of ΔE is achieved.

Mutations in the ENM

We simulate the effect of mutations in our ENM by first supposing that each residue has only one possible mutant – a simplification of the more complex 21 possible amino acids. The mutant residue at each site is either ‘larger’ or ‘smaller’ than the wildtype residue – functionally, this corresponds to a choice of a number $\sigma_i = \pm\sigma$ for each residue, where the sign is randomly chosen. σ_i represents the fractional change in amino acid size upon mutation of residue i .

That is, for a given sequence \mathbf{s} , each rest length l_{ij} is modified from its wildtype value:

$$l_{ij} \rightarrow (1 + \sigma_i)^{s_i} (1 + \sigma_j)^{s_j} l_{ij} \quad (23)$$

We choose $\sigma = 0.1$, corresponding to a roughly 10% difference in size between the wildtype and mutant amino acids.

To compute the deformation upon mutation, we update the rest lengths and then compute the force $\mathbf{f} = -\nabla E_{\text{mut}}(\mathbf{r}_0)$ experienced by the mutant protein in the wildtype configuration \mathbf{r}_0 (where E_{mut} is Eq. 21, with rest lengths given by Eq. 23). Mathematically, this is identical to $-\nabla \delta E(\mathbf{r}_0)$, as defined in 8. The mutation-induced deformation is then computed from Eq. 6.

Fitness functions, double-mutant cycles, and analysis of epistatic matrix

To compute the epistatic matrix, we perform a complete set of double mutant cycles for each simulated elastic network, recording – for each pair of mutants i and j – the structural deformations induced by the single mutants, $\delta_i \mathbf{r}$ and $\delta_j \mathbf{r}$, as well as that elicited by the double mutant, $\delta_{ij} \mathbf{r}$.

We then measure the fitness of each (single or double) mutant by a weighted mean-squared displacement from the wildtype protein:

$$F(\mathbf{r}) \equiv F(\mathbf{r}_0 + \delta \mathbf{r}) = -\frac{1}{N} \sum_{\alpha=1}^N \kappa_{\alpha} |\delta \mathbf{r}_{\alpha}|^2 \quad (24)$$

where $N = 9 \times 9 = 81$ is the number of residues, indexed by α . By construction, the wildtype has fitness 0. We choose each κ_{α} uniformly from the interval $[0, 1]$. Note that the choice of fitness function made here is not essential for our results.

The epistatic co-efficient $\Delta\Delta F_{ij}$ is then computed in the standard way:

$$\Delta\Delta F_{ij} = F(\mathbf{r}_0 + \delta_{ij} \mathbf{r}) - (F(\mathbf{r}_0 + \delta_i \mathbf{r}) + F(\mathbf{r}_0 + \delta_j \mathbf{r}) - F(\mathbf{r}_0)) \quad (25)$$

To give the numbers an appropriate scale, we normalise the epistatic matrix by the average magnitude of the first order mutational effects (i.e. $\langle |\Delta F_i| \rangle$).

To analyse the rank of the epistatic matrix, we first compute $\Delta\Delta F_{ij}^{(1)}$ – a rank-1 approximation of $\Delta\Delta F_{ij}$ – from the singular valued decomposition $\Delta\Delta F = U S V^T$, where S is a diagonal matrix with entries $\{s_1, s_2, \dots\}$, with $s_1 > s_2 > \dots$, as:

$$\Delta\Delta F^{(1)} = U \times \text{diag}(s_1, 0, \dots, 0) \times V^T \quad (26)$$

The matrix $\Delta\Delta F^{(1)}$ is known to be the ‘best’ rank-1 approximation of $\Delta\Delta F$ (i.e. minimises the Frobenius norm of $\Delta\Delta F^{(1)} - \Delta\Delta F$).

We then assessed the complexity of epistasis by computing:

$$\kappa = \frac{\text{median} \left(|\Delta\Delta F_{ij} - \Delta\Delta F_{ij}^{(1)}| \right)}{\langle |\Delta\Delta F_{ij}| \rangle} \quad (27)$$

which is plotted, for each fitness function and each simulated elastic network, in Fig. 2 of the main text.

C. ENM-derived normal mode analysis of PDB structures

Pertaining to Figure 2a of the main text

We compute the normal mode spectrum of a protein from an elastic network model (ENM) built from the PDB structure of the protein. We choose the simplest variant of a ENM; briefly, a unstrained spring with unit spring constant is placed between C- α atoms within 10 angstroms of each other in the crystal structure. The Hessian of the resulting elastic network is computed and diagonalised to obtain the normal mode energies (i.e. the eigenvalues).

D. Relating evolutionary and physical deformations

Pertaining to Figure 2b of the main text

In Fig. 2b we reproduce results from [6], which related the physical deformations of a protein family (as computed from an elastic network based normal mode analysis) to the structural deformations seen between members of a protein family. In particular, we replot:

- **i** The number of principal components required to explain 70% of the structural variation seen across a protein family (quantified from Table 1 in [6], shown in orange in Fig. 2b,i in the main text). As a comparison, we computed the same for a randomly generated dataset of 200 protein family with similar sampling as considered in [6] (i.e. 25 protein structures per family, 100 residues per protein), in which the structural changes of each residue are drawn from a normal distribution with zero mean and unit variance. This is plotted in grey in Fig. 2b,i in the main text.
- **ii** The z-score of the relationship between the top principal components (as defined above) in a protein family, and the lowest normal modes. The plot in Fig. 2b,ii of the main text is obtained by digitising Fig. 6c from [6]; see [6] for details of analysis.

II. GLOBAL AND LOW-RANK EPISTASIS IN PROTEIN ENSEMBLES

A. Theory

Our results above take a mechanical viewpoint of protein function, with a single ground state structure whose low energy vibrational excitations (i.e. its soft mechanical modes) stereotype and simplify epistasis. In contrast, protein function can also be analysed from the point of view of an *ensemble* of protein conformations. Labelling different, discrete conformations by a, b, \dots , the protein is statistically described by a (normalised) ensemble ψ_a , which is the probability of finding the protein in state a .

The function F of a protein may quantitatively be described as $F(\psi_a)$ – that is, different occupancies of the conformational ensemble can change the functional ability of the protein. A classic example is of allostery in hemoglobin, in which allosteric communication from neighbouring hemoglobin molecules shifts an internal equilibrium to alter its affinity for oxygen.

Generally speaking, the distribution ψ_a obeys a master equation of the form:

$$\frac{d\psi_a}{dt} = \sum_{b \neq a} M_{ba} \psi_b - \sum_{b \neq a} M_{ab} \psi_a \quad (28)$$

where M_{ab} is the transition rate from state a to state b . In accordance with detailed balance, the transition rates obey $M_{ab}/M_{ba} = \exp(\beta \Delta E)$, where β is the inverse temperature and $\Delta E \equiv E_a - E_b$ is the difference in energies between states a and b .

By the conservation of probability, and assuming that the ensemble is ergodic, the matrix M_{ab} has a single, unique eigenvector with zero eigenvalue. This eigenvector, $\psi_a^{(\text{WT})}$, is the steady-state (Boltzmann) distribution, describing the native-state thermal ensemble. The remaining eigenvectors, with eigenvalues λ_p , $p \in \{1, \dots\}$, correspond to distinct modes of relaxation to the native-state ensemble, with characteristic rates λ_p . If $|\lambda_1| \ll |\lambda_p|$, any perturbation of the steady state ensemble quickly relaxes to the quasi-steady-state ensemble defined by $\psi_a^{(1)}$, and only then slow relaxes back to the steady state $\psi_a^{(\text{WT})}$.

Consider now the effect of mutations. A single mutation in the protein could alter the energy of each conformation, leading in general to a change in the transition rate matrix $M_{ab} \rightarrow M'_{ab} = M_{ab} + \epsilon \delta M_{ab}$, where we have used the book-keeping variable ϵ to signify a small perturbation. In matrix notation, the new steady state $\vec{\psi}^{(\text{perturb})} = \vec{\psi}^{(\text{WT})} + \epsilon \delta \vec{\psi}$ is, to first order in ϵ :

$$\delta \vec{\psi} = -M^{-1} \left(\delta M \vec{\psi}^{(\text{WT})} \right)$$

where M^{-1} is the pseudo-inverse of M ; more precisely, if the eigendecomposition of M is $Q \Lambda Q^{-1}$, where the columns of Q are the eigenvectors $\vec{\psi}^{(p)}$ and Λ is a diagonal matrix with the eigenvalues λ_p , then:

$$M^{-1} = \sum_{p \geq 1} \frac{1}{\lambda_p} \vec{\psi}^{(p)} \vec{u}_p^T \quad (29)$$

where \vec{u}_p is the p th row of the matrix Q^{-1}

Using the expansion of M^{-1} into eigenmodes, we have

$$\begin{aligned} \delta \vec{\psi} &= - \left(\sum_{\text{modes } p \geq 1} \frac{1}{\lambda_p} \vec{\psi}^{(p)} \left(\vec{\psi}^{(p)} \cdot \delta M \vec{\psi}^{(\text{WT})} \right) \right) \\ &\approx \frac{1}{\lambda_1} \vec{\psi}^{(1)} \underbrace{\left(-\vec{\psi}^{(1)} \cdot \delta M \vec{\psi}^{(\text{WT})} \right)}_{\phi} \end{aligned} \quad (30)$$

where, in analogy with Eq.7, we have defined the mutation-induced perturbation of the ensemble, ϕ . Thus, just as mutations in a mechanical system actuate the low-energy, soft mechanical mode, mutations alter the ensemble of protein conformations along the direction of the slowest relaxational modes of the ensemble. Consequently, as mutations only sample the low-dimensional space defined by $\psi^{(1)}$, the function $F(\vec{\psi})$ reduces to a function of only the scalar variable ϕ , $F(\vec{\psi}) = g(\phi)$. Then, writing the effect of multiple mutations i, j on the transition rates as $\delta M = \delta_i M + \delta_j M + \dots$, we once again obtain global epistasis, with $F(\vec{\psi}) = g(\phi)$, where $\phi = -\sum \vec{\psi}^{(1)} \cdot \delta_i M \vec{\psi}_0$ is the cumulative perturbation of the system to due the mutations i ; see derivation in Sec. 1 for details and for derivation of low-rank epistasis.

III. GLOBAL AND LOW-RANK EPISTASIS IN REGULATORY NETWORKS WITH A SLOW MANIFOLD

A. Theory

Generalising from models of single proteins, we now discuss epistasis in complex genetic, metabolic, or signalling regulatory networks. In each of these systems, the chemical state is specified by a set of expression levels or abundances \mathbf{n} , with an abundance for each of the constituents of the system. In analogy to the molecular coordinates or conformational states of a protein, this is an extremely high-dimensional configuration space which collectively specifies the biological function F performed by the network: $F(\mathbf{n})$. Examples include the net metabolic flux through a cell, or the growth rate as a function of the proteome.

As before, we shall show that if mutations can be made to perturb the steady state of the network along only one dimension, then the resultant epistasis is global and, in a small-perturbation approximation, low-rank.

We begin with a general dynamical system which describes the dynamics of expression levels $\mathbf{n}(t)$ of P components,

$$\frac{\partial}{\partial t} \mathbf{n}(t) = \mathbf{f}(\mathbf{n}) \quad (31)$$

where the (vector) function $\mathbf{f}(\mathbf{n})$ contains terms that describe positive or negative regulation, as well as production and degradation terms. We suppose only that $\mathbf{f}(\mathbf{n})$ depends only on the instantaneous expression level $\mathbf{n}(t)$, and does not have any explicit time-dependence of its own.

Denoting by \mathbf{f}_0 the dynamics of the wildtype regulatory network, the wildtype reaches a steady-state satisfying $\mathbf{f}_0(\mathbf{n}_0) = 0$. The dynamics close to this steady state is described by the Jacobian $\mathcal{J}_0 \equiv \nabla \mathbf{f}(\mathbf{n}_0)$, which plays a role analogous to the Hessian of an elastic network. In particular, the eigenvectors of the Jacobian, \hat{v}_m ($m \in \{0, \dots, P-1\}$), describe the relaxational modes of the system. The eigenvalues λ_m determine the timescales of relaxation of each mode.

Analogous to a soft mechanical mode is a slow relaxational mode, defined by $|\lambda_0| \ll \lambda_m$ for $m > 0$, associated with a *slow manifold* defined by the eigenvector \hat{v}_0 . Slow modes describe the long-time dynamics of relaxation to the steady state – an initially perturbed system will relax quickly to the slow manifold, and only then relax slowly back to the steady state with timescale $-1/\lambda_0$. See [7–9] for a description of how slow manifolds could arise in evolved regulatory networks.

Note that, if there is a single slow mode, λ_0 is by necessity real. Therefore, while we shall use λ_m in this section to denote the (potentially complex) eigenvalue itself, in the main text and elsewhere in the SI we shall use λ_m to denote only its real part (the so-called *Lyapunov exponent*).

Mutations, or sustained external perturbations such as a change in nutrients, modify the regulatory dynamics $\mathbf{f}_0(\mathbf{n}) \rightarrow \mathbf{f}_0(\mathbf{n}) + \delta \mathbf{f}(\mathbf{n})$. We shall suppose that multiple mutations i and j alter the regulatory dynamics as $\delta \mathbf{f} = \delta_i \mathbf{f} + \delta_j \mathbf{f}$, as would be expected for mutations that perturb different components or physical processes of a network [10, 11]. The new steady state $\mathbf{n}_0 + \delta \mathbf{n}$ satisfies

$$\mathbf{f}_0(\mathbf{n}_0 + \epsilon \delta \mathbf{n}) + \epsilon \delta \mathbf{f}(\mathbf{n}_0 + \epsilon \delta \mathbf{n}) = 0 \quad (32)$$

where we have introduced the book-keeping variable ϵ to indicate that the perturbation $\delta \mathbf{f}$ is small. To first order in ϵ :

$$\delta \mathbf{n} \approx -\mathcal{J}_0^{-1} \delta \mathbf{f}(\mathbf{n}_0) \approx \frac{1}{\lambda_0} \underbrace{(-\hat{v}_0 \cdot \delta \mathbf{f})}_{\phi} + \mathcal{O}\left(\frac{1}{|\lambda_1|}\right) \quad (33)$$

where in the last step we have invoked the existence of a slow manifold, and defined the mutation-induced perturbation ϕ , in analogy with Eq. 7 for the mechanical networks. Thus, mutations in the background of a slow manifold \hat{v}_0 perturb the system primarily along the slow manifold. Consequently, exactly as we have described for proteins, epistasis between mutations will be global; see derivations above for details.

B. Numerical methods

Model

We simulate a family of regulatory networks with $P = 30$ species ('genes') whose expression levels n_a , $a \in \{1, \dots, M\}$, evolve as:

$$\frac{\partial}{\partial t} n_a = \sum_b k_{ab} \frac{n_b}{n_b + K_{ab}} - \lambda_a n_a \quad (34)$$

where, as described in the main text, K_{ab} , k_{ab} parameterise the regulation $b \rightarrow a$, and λ_a is the decay-rate for species a . The choice of these parameters completely specify the particular regulatory network.

For simplicity, we set the decay rates of all species a to $\lambda_a = 5$, which sets the units of time in the simulation. Eq. 34 is solved by the Euler method with time-step $\Delta t = 0.01$. Given initial conditions, the steady state \mathbf{n}_0 is found by solving the equation until the change in each species n_a over a unit interval of time is less than a specified tolerance (here, 10^{-7}).

Varying the gap in the Lyapunov spectrum

To obtain a regulatory network with a specified gap in its Lyapunov spectrum, we begin with a randomly generated regulatory network. Explicitly, we first choose which of the 435 possible regulatory edges to include in the network, by including each with a probability $p = 0.3$ (i.e., giving a directed Erdos-Renyi graph). Then, for each included regulatory edge, the values of the constants K_{ab} and k_{ab} is set by sampling uniformly over the unit interval, resulting in a fully specified random regulatory network.

The steady state is found by solving the equations of motion, Eq. 34, with initial conditions $n_a = 0.5$; diagonalising the Jacobian \mathcal{J}_0 around the steady state, we obtain the (sorted) Lyapunov exponents λ_i as the negative of the real part of the eigenvalues. Our quantity of interest is the gap between the first two exponents:

$$\Delta\lambda \equiv \frac{\lambda_1}{\lambda_0} \quad (35)$$

For the initially random regulatory networks, we find that $\Delta\lambda \sim 1.5$.

We then use a Monte Carlo algorithm to obtain networks with varying $\Delta\lambda$. Briefly, at each step of the algorithm, a single regulatory edge $b \rightarrow a$ is chosen, and its parameters k_{ab} , K_{ab} are perturbed by an amount uniformly distributed in $[-0.2, 0.2]$. Parameters are not allowed to become negative, or to grow greater than 1. The steady state and Lyapunov spectrum of the new network is computed, and the change in parameters accepted if:

1. The gap $\Delta\lambda$ increases
2. The inverse participation ratio, defined in terms of the elements of the lowest eigenvector v_a as:

$$\text{IPR} = \sum_{i=1}^P (v_a v_a^*)^2 \quad (36)$$

decreases or is already below $2/P$, where $P = 30$ is the total number of species in the network.

The algorithm terminates when the desired mode gap is reached. We generated a total of 320 regulatory networks, the results of which (as detailed in the next section) are shown in Figure 3 in the main text.

Mutations, fitness, and epistasis

For each network, the effect of $M = 50$ single mutations (and their double mutants) is simulated, and the epistatic matrix $\Delta\Delta F_{ij}$ computed. Each mutation i is taken to affect a single regulatory edge $b \rightarrow a$ – representing, for instance, mutations in the domain of species b responsible for regulating a . The set of M mutants is chosen by computing the 'regulatory strength' $k_{ab}n_b/(K_{ab} + n_b)$, at the wildtype steady state, for each edge and choosing the top M . The effect of each mutation is to increase or decrease k_{ab} and K_{ab} (for the regulatory edge associated with that mutation) by 10%; the new steady state $\mathbf{n} = \mathbf{n}_0 + \delta\mathbf{n}$ is found by solving Eq. 34 initialised at the wildtype fixed point \mathbf{n}_0 .

We choose as a fitness function the following:

$$F(\mathbf{n}) = \exp\left(-\frac{1}{2}(\mathbf{n} - \mathbf{n}_0)^T \mathcal{K} (\mathbf{n} - \mathbf{n}_0)\right) \quad (37)$$

where \mathbf{n} is the steady state of the mutated network, and \mathbf{n}_0 is the wildtype steady state. The matrix \mathcal{K} is chosen randomly to realise different randomly generated fitness functions (plotted as different symbols in Fig.3 of the main text).

The epistatic matrix, its rank-1 approximation, and the epistatic complexity κ is then computed just as for the elastic network simulation.

C. Principal component analysis of *E. coli* proteomics data

A key consequence of the existence of a slow manifold in a regulatory network is a low-dimensional response to perturbations, be they mutations or a change in external condition. We tested this with data from the experiments of [12], as obtained from data the repository in [13]. The dataset consists of protein copy number in *E. coli* quantified across 17 different growth conditions (the dataset originally consisted of 19 conditions; however, we excluded two stationary phase measurements from the analysis). After excluding proteins whose copy number were below the quantitation limit in any one condition, we end up with 1971 protein copy numbers quantified across growth conditions. We perform principal component analysis on this dataset, the results of which are plotted in orange in Fig. 3c of the main text. As a control, we randomly scrambled the copy numbers across conditions and protein labels, resulting in the grey data points in Fig. 3c in the main text.

IV. LOW-RANK EPISTASIS AND EVOLUTIONARY RUGGEDNESS

To gauge the evolutionary implications of low-rank epistasis, we carried out a simple numerical calculation to assess the ruggedness of a fitness landscape with a tunable rank of epistasis. For simplicity, we choose a fitness landscape with only second-order epistasis:

$$F(\mathbf{s}) = \sum_i \Delta F_i s_i + \sum_{i>j} \Delta\Delta F_{ij} s_i s_j \quad (38)$$

where, as earlier, $s_i \in \{0, 1\}$, for i between 1 and the sequence length L , specifies the genotype, and ΔF_i , $\Delta\Delta F_{ij}$ are the first and second order epistatic coefficients, respectively. We parameterise $\Delta\Delta F_{ij}$ as:

$$\Delta\Delta F_{ij} = (1 - \kappa) \theta_i \theta_j + \kappa J_{ij} \quad (39)$$

where J_{ij} is a symmetric, full-rank matrix. The variable κ is the epistatic complexity, comparable to the definition in Eq. 27, which tunes $\Delta\Delta F_{ij}$ from rank-1 ($\kappa = 0$) to full-rank ($\kappa = 1$).

We simulate greedy adaptive walks in the landscape Eq. 38. At each step, the mutation that leads to the largest gain in fitness is chosen. The simulation is terminated when the population reaches a local fitness maximum, i.e. when all mutations are deleterious.

We use a genome length of $L = 50$, and sample κ in steps of 0.05 between 0 and 1. For each κ , 100 random fitness landscapes are generated, by sampling ΔF_i , θ_i , and J_{ij} from a normal distribution with mean 0 and variance 1. For each landscape, 100 adaptive walks are performed starting from random initial conditions, and the number of unique fitness maxima reached is recorded. This, averaged over landscapes, is plotted (along with its standard deviation), in Fig. 4 of the main text.

-
- [1] Jakub Otwinowski, David M. McCandlish, and Joshua B. Plotkin. Inferring the shape of global epistasis. *Proceedings of the National Academy of Sciences of the United States of America*, 115(32):E7550–E7558, 2018.
 - [2] Sandipan Dutta, Jean Pierre Eckmann, Albert Libchaber, and Tsvi Tlusty. Green function of correlated genes in a minimal mechanical model of protein evolution. *Proceedings of the National Academy of Sciences of the United States of America*, 115(20):E4559–E4568, 2018.
 - [3] Le Yan, Riccardo Ravasio, Carolina Brito, and Matthieu Wyart. Architecture and coevolution of allosteric materials. *Proceedings of the National Academy of Sciences of the United States of America*, 114(10):2526–2531, mar 2017.

- [4] Jason W. Rocks, Nidhi Pashine, Irmgard Bischofberger, Carl P. Goodrich, Andrea J. Liu, and Sidney R. Nagel. Designing allosteric-inspired response in mechanical networks. *Proceedings of the National Academy of Sciences of the United States of America*, 114(10):2520–2525, mar 2017.
- [5] Ivet Bahar, Timothy R. Lezon, Ahmet Bakan, and Indira H. Shrivastava. Normal mode analysis of biomolecular structures: Functional mechanisms of membrane proteins. *Chemical Reviews*, 110(3):1463–1497, 2010.
- [6] Alejandra Leo-Macias, Pedro Lopez-Romero, Dmitry Lupyan, Daniel Zerbino, and Angel R. Ortiz. An analysis of core deformations in protein superfamilies. *Biophysical Journal*, 88(2):1291–1299, feb 2005.
- [7] Kunihiko Kaneko, Chikara Furusawa, and Tetsuya Yomo. Universal relationship in gene-expression changes for cells in steady-growth state. *Physical Review X*, 5(1), 2015.
- [8] Chikara Furusawa and Kunihiko Kaneko. Formation of dominant mode by evolution in biological systems. *Physical Review E*, 97(4):42410, 2018.
- [9] Kunihiko Kaneko and Chikara Furusawa. Macroscopic Theory for Evolving Biological Systems Akin to Thermodynamics. *Annual Review of Biophysics*, 47(1):273–290, may 2018.
- [10] Daniel Segrè, Alexander DeLuna, George M. Church, and Roy Kishony. Modular epistasis in yeast metabolism. *Nature Genetics*, 37(1):77–83, jan 2005.
- [11] Griffin Chure, Manuel Razo-Mejia, Nathan M. Belliveau, Tal Einav, Zofia A. Kaczmarek, Stephanie L. Barnes, Mitchell Lewis, and Rob Phillips. Predictive shifts in free energy couple mutations to their phenotypic consequences. *Proceedings of the National Academy of Sciences*, 116(37):18275–18284, sep 2019.
- [12] Alexander Schmidt, Karl Kochanowski, Silke Vedelaar, Erik Ahrné, Benjamin Volkmer, Luciano Callipo, Kèvin Knoops, Manuel Bauer, Ruedi Aebersold, and Matthias Heinemann. The quantitative and condition-dependent Escherichia coli proteome. *Nature Biotechnology*, 34(1):104–110, jan 2016.
- [13] Uri Barenholz, Leeat Keren, Eran Segal, and Ron Milo. A minimalistic resource allocation model to explain ubiquitous increase in protein expression with growth rate. *PLoS ONE*, 11(4):e0153344, apr 2016.